ResearchGate

See discussions, stats, and author profiles for this publication at: https://www.researchgate.net/publication/263959897

Electrostatic Control of Orbital Ordering in Noncubic Crystals

ARTICLE *in* THE JOURNAL OF PHYSICAL CHEMISTRY C · MARCH 2014

Impact Factor: 4.77 · DOI: 10.1021/jp412329x

CITATIONS
4

READS
32

3 AUTHORS, INCLUDING:

Miguel Moreno
Universidad de Cantabria
224 PUBLICATIONS **2,736** CITATIONS

SEE PROFILE

Available from: Miguel Moreno
Retrieved on: 02 February 2016

THE JOURNAL OF PHYSICAL CHEMISTRY C

Article

pubs.acs.org/JPCC

Electrostatic Control of Orbital Ordering in Noncubic Crystals

Pablo García-Fernández,* Miguel Moreno, and José A. Aramburu

Departamento de Ciencias de la Tierra y Física de la Materia Condensada, Universidad de Cantabria, Avenida de los Castros s/n, 39005 Santander, Spain

Supporting Information

ABSTRACT: In noncubic insulating crystals where active orbitals are not degenerate the usual models to describe orbital ordering, Kugel–Khomskii and Jahn–Teller, are, in principle, not valid. For these materials we show, by means of first-principles calculations, that a key driving force behind orbital ordering is the electrostatic potential, $V_R(\mathbf{r})$, created by the rest of lattice ions over the magnetic complex where active electrons are localized. In order to illustrate the key influence of $V_R(\mathbf{r})$, often ignored in a true microscopic approach, we focus on K_2CuF_4 and La_2CuO_4 as model crystals since they have very similar electronic structure but, surprisingly, contrasting orbital orderings, antiferrodistortive and ferrodistortive, respectively. Considering the parent K_2NiF_4 structure (tetragonal space group $I4/mmm$) of both lattices, it is shown that in K_2CuF_4 the hole in a CuF_6^{4-} complex is forced by the anisotropy of $V_R(\mathbf{r})$ to be in a $3z^2 - r^2$ orbital, while for La_2CuO_4 the shape of $V_R(\mathbf{r})$ forces the hole to be placed in the planar $x^2 - y^2$ orbital. As a salient feature, it is found that in the parent structure the orbitals of K_2CuF_4 are ferrodistortively ordered in contrast to the Kugel–Khomskii prediction. At the same time, it is also shown that in K_2CuF_4 this state is unstable and distorts to the experimental antiferrodistortive state where, despite the significant in-plane distortion, the hole is still found to be in a mainly $3z^2 - r^2$ orbital, a fact in agreement with experimental magnetic resonance data. For this compound, it is found that $V_R(\mathbf{r})$ induces changes on the energy of 3d levels, which are 2 orders of magnitude higher than those due to superexchange interactions. The present results stress that in insulating transition metal compounds with electrons localized on complexes the rest of the lattice ions play a key role for understanding the electronic and structural properties that is, in many cases, overlooked. The present ideas are also shown to account for the orbital ordering in other noncubic materials, like Na_3MnF_6, $NaCrF_4$, or $Sr_2La_2CuTi_3O_{12}$, and thus open a window in the design of magnetic materials.

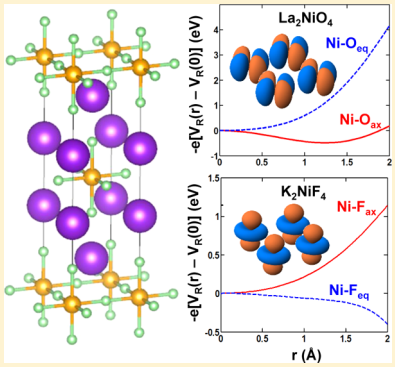

I. INTRODUCTION

The current interest in transition-metal oxides and their interfaces largely lies in the strong correlation and competition existing between several of their degrees of freedom, yielding phases with unique properties that are very close in energy.[1,2] In particular, the orbital degree of freedom is especially relevant when determining the structure and magnetism of these systems,[1−4] and key materials like the colossal magnetoresistance manganites[3] show a spatial ordering of the electrons and holes strongly localized in the anisotropic d-shell orbitals. Hence, obtaining reasonable models that allow describing these systems and provide an intuition in how they work can be very important from the point of view of material design.

A first model to explain the structure of orbital ordering (OO) systems was given by Kanamori in the sixties[5] showing that, in insulating crystals where ions have degenerate semioccupied orbitals, the electron–phonon coupling in the form of local Jahn–Teller (JT) distortions[6,7] of interacting neighboring sites produces long-range structural order. Kanamori proposed a first classification of the different types of OO by analogy with magnetism: distortions that align in the same way at all sites of the lattice were called ferrodistortive (FD) while those that produce a staggered pattern are antiferrodistortive (AFD) (see Figure 1). A second, fundamental contribution in the field was given by Kugel and Khomskii (KK) who showed that superexchange between electrons occupying *degenerate* orbital shells[8,9] also leads to cooperative orbital interactions, and within the model, the resulting crystal distortions are simply a consequence of the *preexisting* OO. A main advantage of this approach compared to the JT one is that the resulting magnetic state of the system is an integral part of the theory.

Archetypical systems where these models have been applied are $KCuF_3$ and $LaMnO_3$ perovskites. Both crystals display an AFD distortion (although of slightly different kind due to the presence of octahedral tilting in $LaMnO_3$) and an antiferromagnetic (AFM) ground state[10,11] consistent with the application of the KK model over a *cubic* perovskite structure.[8,9] Recent ab initio calculations carried out to determine, in a rigorous way, the relative value of JT and exchange effects show that both contributions are similarly important.[12,13]

Arguably, a more interesting situation arises when one compares layered-perovskite analogues of the previous lattices, K_2CuF_4 and La_2CuO_4, whose crystal structures are shown in

Received: December 17, 2013
Revised: March 21, 2014
Published: March 21, 2014

 © 2014 American Chemical Society dx.doi.org/10.1021/jp412329x | J. Phys. Chem. C 2014, 118, 7554–7561

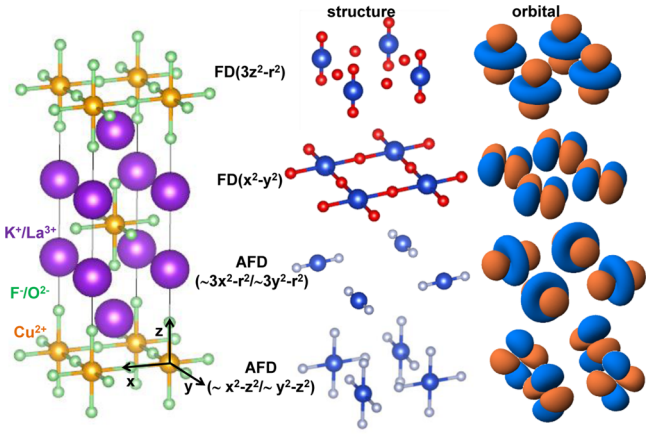

Figure 1. Left: $I4/mmm$ K_2NiF_4 structure parent of the orbitally ordered lattices K_2CuF_4 and La_2CuO_4. Right: four primary types of orbital orderings, considered in this work, as schematically represented by the unoccupied orbitals and their associated structures for the 2D $Cu(F,O)_2$ planes (bonds are only plotted to first neighbors). The symbol "~" preceding in-plane orbitals ($\sim 3x^2 - r^2/\sim 3y^2 - r^2$, and $\sim x^2 - z^2/\sim y^2 - z^2$) denotes that these orbitals do not have the pure character shown in their notation as these wave functions have an orthorhombic perturbation since they are not oriented along the tetragonal axis of the crystal (see discussion in main text).

Figure 2. Both insulating compounds have the *same parent* structure, which is that displayed by the tetragonal K_2NiF_4 and

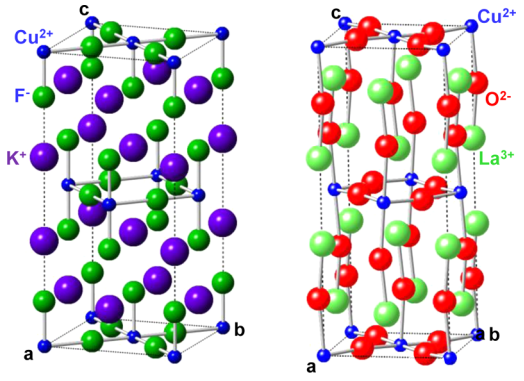

Figure 2. Equilibrium crystal structures of K_2CuF_4 (left) and La_2CuO_4 (right) lattices with the usual axes notation of the nonstandard *Bbcm* space group that allows placing the **c** axis along z as in the case of the $I4/mmm$ reference structure (see Figure 1).

La_2NiO_4 lattices (space group $I4/mmm$), where the principal C_4 axis lies along the crystallographic **c** axis (Figure 1). Since both systems have the same reference structure and their electronic configuration is very similar one would expect, at first sight, no qualitative difference in their properties. However, these compounds exhibit very different behaviors. K_2CuF_4 is a ferromagnet (FM) that displays an AFD distortion[14] in the plane perpendicular to the **c** axis. More precisely, in K_2CuF_4 the CuF_6^{4-} complexes have a *long* Cu^{2+}–F^- bond (R_L = 2.223 Å) in the plane perpendicular to the **c** axis, while the two other pairs of *short* bonds are *nearly* equal with R_S = 1.900 Å (in-plane) and 1.937 Å (out-of-plane) (Table 1). Owing to this fact it has widely been *assumed* that the main axis for CuF_6^{4-} complexes in K_2CuF_4 lies in the plane perpendicular to the **c** axis such as it would happen for an *isolated* CuF_6^{4-} unit. According to this view $\sim 3y^2 - r^2$ or $\sim 3x^2 - r^2$ orbitals of CuF_6^{4-} in K_2CuF_4 are

Table 1. Optimized vs Experimental Crystal Structure Parameters for K_2CuF_4 and La_2CuO_4 Compounds[a]

system	group	a	b	c	R (2x,2x,2x)
K_2CuF_4	*Bbcm*	5.832	5.832	12.746	1.900, 1.937, 2.223
		5.904	*5.904*	*12.734*	*1.939, 1.941, 2.234*[b]
K_2CuF_4	*I4/mmm*	4.121	4.121	12.537	1.906, 2.061, 2.061
La_2CuO_4	*Bbcm*	5.323	5.330	13.182	1.884, 1.884, 2.392
		5.402	*5.361*	*13.155*	*1.905, 1.905, 2.413*[c]
La_2CuO_4	*I4/mmm*	3.777	3.777	13.375	1.889, 1.889, 2.415

[a]Optimized values (first row) compared with experimental data (second row, italic letters) of the lattice parameters **a**, **b**, and **c** (in Å units) and Cu–F/O distances (in Å), R. Calculated values for the *Bbcm* equilibrium structure and the *I4/mmm* parent structure are both reported. [b]Experimental data from ref 14. [c]Experimental data from ref 15.

doubly occupied, while the hole resides in $\sim x^2 - z^2/\sim y^2 - z^2$ orbitals. For a pure tetragonal CuF_6^{4-} complex such orbitals involve 75% and 25% of $3z^2 - r^2$ and $x^2 - y^2$ character, respectively. It will be shown that this description, though widely accepted, is subtly but importantly modified, when the influence of the rest of the lattice ions upon a CuF_6^{4-} complex is considered.

On the contrary, La_2CuO_4 is notorious for being a strong AFM[15] and has an axial FD structure with a doubly occupied $3z^2 - r^2$ orbital and a hole in $x^2 - y^2$. In this case the long axis of CuO_6^{4-} complexes lies along the **c** axis of the parent structure and R_L = 2.392 Å (two bonds out-of-plane) and R_S = 1.884 Å (four bonds in-plane) (Table 1). The OO in La_2CuO_4 can be denoted as FD($x^2 - y^2$). It is important to note that, apart from a small tilting, this orbital is perfectly aligned with the main axis of the crystal, at difference with the experimental situation in K_2CuF_4, and thus, the hole belongs to a *pure* $x^2 - y^2$ state.

The OO in K_2CuF_4 has been largely attributed to KK interactions[8,9] even though the correct ground state is only reached after taking into account the charge-transfer nature of the insulating state.[16] However, the situation is less clear for La_2CuO_4, which is the parent system of high-Tc superconducting cuprates. In this case both strong localization effects[17] and the two-dimensional nature of the lattice jointly with a strong JT effect[3] have been attributed to be responsible for the localization of the hole in the $x^2 - y^2$ orbital. However, these arguments do not explain a crucial experimental fact: why these two systems, that in appearance are so similar, behave in such different ways. In particular it seems reasonable that if the KK model is applicable to K_2CuF_4 it should also be applied to La_2CuO_4. Reciprocally, since K_2CuF_4 has a 2D nature and large JT-like distortions, why are the ground state and structure so different to that of La_2CuO_4 (see Table 1)? The reason is not the large magnitude of the local JT-like distortion since the experimental ratio R_L/R_S is equal to 1.15 in the fluoride[14] compared to 1.27 in the oxide.[15]

In this work we show that the strong difference in the OO of these, a priori, similar lattices is due to the disparate electrostatic nature of both crystals. In fact, we will demonstrate that, in contrast with the short-range interaction models discussed above, the main factor determining the OO type for a large class of magnetic systems is the long-range electric field created by the lattice over each transition-metal complex where

dx.doi.org/10.1021/jp412329x | J. Phys. Chem. C 2014, 118, 7554–7561

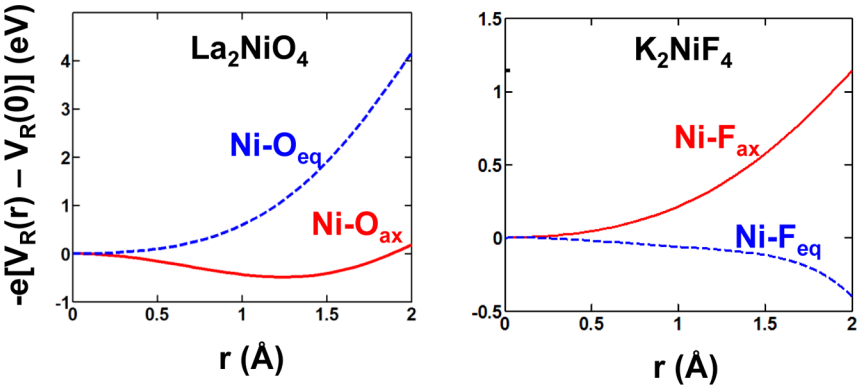

Figure 3. $(-e)\{V_R(\mathbf{r}) - V_R(0)\}$ potential energy felt by an electron of a NiL_6 complex (L = O, F) for La_2NiO_4 and K_2NiF_4 parent structures of La_2CuO_4 and K_2CuF_4, respectively. Energies are depicted along the axial M−L_{ax} direction, parallel to the crystallographic c axis (solid red lines) and along in-plane equatorial M−L_{eq} (dashed blue lines) bond directions.

active electrons are *localized*. It will be shown that a great help for understanding the actual electronic and geometrical structure of K_2CuF_4 and La_2CuO_4 is obtained studying the behavior of Cu^{2+} complexes under the electric field in the corresponding *parent structure* (K_2NiF_4 or La_2NiO_4) both of which exhibit the *same* $I4/mmm$ space group. The associated potential, $V_R(\mathbf{r})$, which has been shown to be crucial in the determination of spectroscopic features of layered systems,[18] allows determining under which circumstances a particular OO pattern may arise and thus can be useful for solid-state chemists to produce systems with specially designed properties. In order to support these ideas we have carried out first-principles density functional theory (DFT) calculations using hybrid-functionals.[19,20] Aside from La_2CuO_4 and K_2CuF_4, calculations have also been carried out on other insulating compounds like $NaCrF_4$, Na_3MnF_6, or $Sr_2La_2CuTi_3O_{12}$, which will be discussed in a second step.

This work is arranged as follows. A short account of computational details is given in the next section, while the results of this work are subsequently exposed. Main conclusions are summarized in the last section.

II. COMPUTATIONAL DETAILS

We performed first-principles calculations using density functional theory and hybrid exchange-correlation functionals. In particular we employed B1WC[20] and PW1PW[21] functionals containing, respectively, 16% and 20% of Hartree−Fock exchange. Both functionals display excellent performance being able to very accurately predict structural, thermochemical, and magnetic properties in oxides.[22,23] In particular, ab initio simulations using these techniques have shown high accuracy in the simulation of perovskite crystals capturing, to a high degree, the strong electron correlation in these systems *without the need* to introduce semiempirical parameters for each system like in LDA+U or GGA+U calculations.

We employed the CRYSTAL09 code[19] combined with double-ζ[24] and high quality triple-ζ[25] basis-sets. Our calculations were carried out employing a crystal cell corresponding to the conventional $I4/mmm$ cell expanded to a $\sqrt{2} \times \sqrt{2} \times 1$ supercell in order to be able to accommodate various magnetic orderings. The reciprocal space was sampled with a $8 \times 8 \times 6$ net. The parameters controlling the accuracy of integration of Coulomb and exchange parameters were set to 9, 9, 9, 9, and 18 and the energy convergence to 10^{-9} hartree, and an extra-large grid was used for spatial integration of the electron density. Very tight criteria for optimizations were imposed. In particular, the tolerances for energy, gradients, and displacements were, respectively, 10^{-9} hartree, 0.00003, and 0.00012.

During the calculation of $I4/mmm$ phases of orbitally ordered systems we tried several initial configurations to determine which one converged to the state with lowest energy. Using the $\sqrt{2} \times \sqrt{2} \times 1$ supercell described above, containing two Cu centers per plane of the lattice, we started with ferrodistortive configurations where the holes in both Cu^{2+} ions were in the same orbital (either $3z^2 - r^2$ or $x^2 - y^2$) or antiferrodistortive where the hole is in different positions as expected from the Kugel−Khomskii model.

III. RESULTS AND DISCUSSION

We will now proceed to describe our model for K_2CuF_4 and La_2CuO_4 compounds, which is separated in two steps. In the first step we show that the effect of the internal electric field of the *parent* K_2NiF_4-type lattice stabilizes either FD($x^2 - y^2$) or FD($3z^2 - r^2$) states. In the second one we demonstrate through ab initio calculations that the FD($3z^2 - r^2$) state is unstable and decays, giving rise to an antiferrodistortive pattern.

Electrostatic Potential of K_2NiF_4 and La_2NiO_4 Parent Lattices. In our first step we start with the calculation of the electrostatic potential, $V_R(\mathbf{r})$, over a particular magnetic ML_6 complex (M = transition metal cation; L = ligand) due to the rest of the ions of the lattice, assuming that the crystal structure is that of a high-symmetry parent compound that does not display OO. For example, in the case of K_2CuF_4 and La_2CuO_4 the parent geometry would correspond to the tetragonal $I4/mmm$ group displayed by *both* K_2NiF_4 and La_2NiO_4 compounds. While the reference structure is the same for both lattices, the internal electrostatic field is, however, notably different since the charges of ions[25] involved in K_2NiF_4 and La_2NiO_4 are not the same.

Using, for example, the Ewald method it is easy to obtain the electrostatic potential, $V_R(\mathbf{r})$, observed by an electron localized around the Ni-site along the main directions (x,y,z) to where the sigma ($x^2 - y^2$, $3z^2 - r^2$) orbitals are directed. This is shown in Figure 3 for the parent lattices K_2NiF_4 and La_2NiO_4. In the first case, the in-plane (x,y) potential quickly descends, while the one along the z direction (parallel to the crystallographic **c** axis) ascends, favoring the localization of electrons in the equatorial $x^2 - y^2$ orbital and the displacement of the unpaired hole to the $3z^2 - r^2$ orbital. However, the opposite behavior is observed for La_2CuO_4 where the hole is pushed toward the

dx.doi.org/10.1021/jp412329x | J. Phys. Chem. C 2014, 118, 7554−7561

plane. The origin of the different behavior of $\{V_R(\mathbf{r}) - V_R(\mathbf{0})\}$ in K_2NiF_4 and La_2NiO_4 can qualitatively be found just inspecting the charge of the second neighbor of the transition metal along the main axes of the parent crystal (Figure 2). While in both cases the second neighbor of the Cu^{2+} ion in the *x,y*-plane is a transition metal of the same kind, there are important differences in the axial second neighbor. On one hand, the second neighbor in the *z* direction in the oxide is a La^{3+} ion, which attracts electrons toward the axis more strongly that the Cu^{2+} ions in the plane, stabilizing a FD($x^2 - y^2$) phase. On the other hand, the axial neighbor in the fluoride is a K^+ ion whose charge cannot compensate that Cu^{2+} ions in plane and thus two electrons will be in the planar $x^2 - y^2$ orbital and only one in the highest $3z^2 - r^2$ one thus giving rise, in principle, to a FD($3z^2 - r^2$) phase.

To quantify this effect we have performed calculations, following the procedure of ref 18, for an *isolated* CuF_6^{4-} complex at R_L = 1.997 Å (in-plane) and R_S = 1.982 Å (out-of-plane), corresponding to the idealized K_2NiF_4 structure, finding that the separation between $x^2 - y^2$ and $3z^2 - r^2$ orbitals is equal *only* to 0.06 eV. By contrast, the value of this splitting becomes *six times* higher when the CuF_6^{4-} complex is also allowed to feel the action of $V_R(\mathbf{r})$ coming from the K_2NiF_4 lattice. Thus, the situation changes from near degeneracy without the $V_R(\mathbf{r})$ potential, where JT or KK models are dominant, to the other where the separation between both states is much larger than the typical JT energy in oxides/fluorides (usually smaller[12,13,18,26] than 0.1 eV) or the superexchange energy acting in KK. In order to give some numerical estimates of the superexchange energy we would like to note that in a system with electron degeneracy like $KCuF_3$ where superexchange is very strong, it only amounts[12] to 0.03 eV, which is much smaller than the energy splitting induced by $V_R(\mathbf{r})$. Moreover, superexchange is weaker in K_2CuF_4 than in $KCuF_3$ as seen from a reduction in the magnetic transition temperature in more[27,28] than a factor of 6. It is also noteworthy that nuclear magnetic resonance experiments on ^{19}F nuclei[27] in K_2CuF_4 strongly suggest that the unpaired electron is placed on an orbital with a dominant $3z^2 - r^2$ character, a result fully consistent with the present view.

Thus, in the first step of our reasoning we predict that La_2CuO_4 will condensate to a FD($x^2 - y^2$) state, while K_2CuF_4 to a FD($3z^2 - r^2$) one. In order to find how strong this condensation is we have carried out geometry optimizations calculations for these lattices under the *I*4/*mmm* group describing the K_2NiF_4 structure, and the structural parameters are given in Table 1. For K_2CuF_4 and La_2CuO_4, the energies of the optimized *I*4/*mmm* structures are, respectively, 0.096 and 0.491 eV per formula *greater* than those corresponding to the *Bbcm* structures. It must be noted, however, that the distortion of these systems is very different. For K_2CuF_4 a coordinated elongated/contraction of the equatorial Cu−F bonds is produced, consistent with a change in the nature of OO. However, in La_2CuO_4 this distortion is not observed (see Table 1) although a buckling of the CuO_2 plane is produced due to the tilting of the CuO_6 octahedra leaving the original OO unchanged. As a salient feature in both cases the hole in the *I*4/*mmm* group is found to be almost completely localized (over 95%) on a specific type of orbital (Figure 4), showing that the KK mechanism for OO in K_2CuF_4 is absent as the orbitals *are not* AFD *ordered* for the high-symmetry parent structure.[8,9,16] This fact was checked in several ways. The lowest FM and AFM states were calculated, both showing a similar behavior with

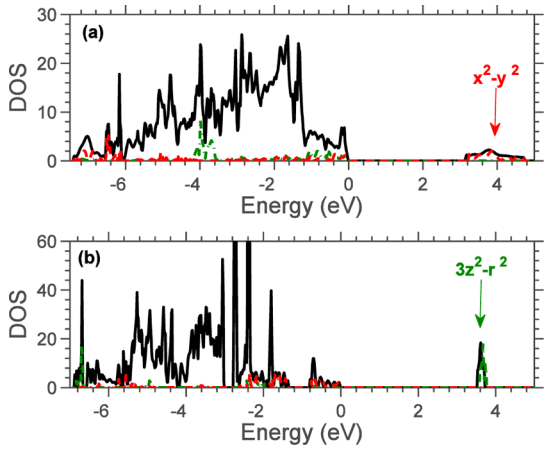

Figure 4. Solid black lines: Total DOS (sum of spin-up and spin-down) of La_2CuO_4 (a) and K_2CuF_4 (b) for the *I*4/*mmm* structures. Projections over Cu($x^2 - y^2$) and Cu($3z^2 - r^2$) orbitals are displayed with dashed red lines and dash−dot green lines, respectively. Arrows show the character of the highest occupied band.

respect to OO. Similarly, convergence in some simulations was started with an initial orbital occupation consistent with an AFD ordering but the lowest-energy state found for the *I*4/*mmm* structure is always FD($3z^2 - r^2$) (see computational details). These results are also consistent with experiments[29] and calculations[30] carried out on layered fluorides containing Cu^{2+} *impurities*. For instance, in Cu^{2+}-doped K_2ZnF_4, CuF_6^{4-} complexes exhibit a tetragonally compressed geometry along the **c** axis with the unpaired electron placed in the $3z^2 - r^2$ orbital due to the electric field from the rest of the lattice.[30] As a consequence and as explained in a step two of our analysis, it is necessary to move beyond the KK mechanism to explain the nature of the ground state in K_2CuF_4 and the origin of the in-plane distortion of the ligands.

Instability of the FD($3z^2 - r^2$) State in K_2CuF_4. In the second step of our model we will show how the FD($3z^2 - r^2$) state in K_2CuF_4 is unstable. Experimentally, there are many systems that are FD($x^2 - y^2$) type, for example, Na_3MnF_6, $CuWO_4$, or $Sr_2La_2CuTi_3O_{12}$ (see below), but very few in the FD($3z^2 - r^2$) phase as crystals like K_2CuF_4 usually further distort to an AFD state. It is important, then, to study in a first step the stability of the FD($x^2 - y^2$) state with respect to the FD($3z^2 - r^2$) one. To do so, we consider the electrostatic potentials, $V_R(\mathbf{r})$, shown in Figure 3, noting that they not only affect the movement of electrons but *also* produce forces over the negatively charged ligands. In La_2CuO_4 the FD($x^2 - y^2$) state orientates the doubly occupied Cu($3z^2 - r^2$) antibonding orbital toward the axial ligands pushing them closer to the La^{3+} ion in a JT-like distortion, a movement that is energetically favorable and effectively pins the position of these anions (see Table 1). Moreover, a look at the potentials depicted in Figure 3 for La_2NiO_4 shows that in La_2CuO_4 an AFD distortion where the long axial distance is reduced to elongate an equatorial one is electrostatically unfavorable. Therefore, in La_2CuO_4 and similar systems the FD($x^2 - y^2$) state is electrostatically stable.

A very different situation arises when one considers the FD($3z^2 - r^2$) configuration in K_2CuF_4 where we find three main causes for the instability: (a) While in La_2CuO_4 the electrostatic potential, $V_R(\mathbf{r})$, stabilizes *both* the FD($x^2 - y^2$) state and the distortion; in the case of K_2NiF_4, the in-plane potential (Figure 3) is nonlinear and quickly descending

dx.doi.org/10.1021/jp412329x | J. Phys. Chem. C 2014, 118, 7554−7561

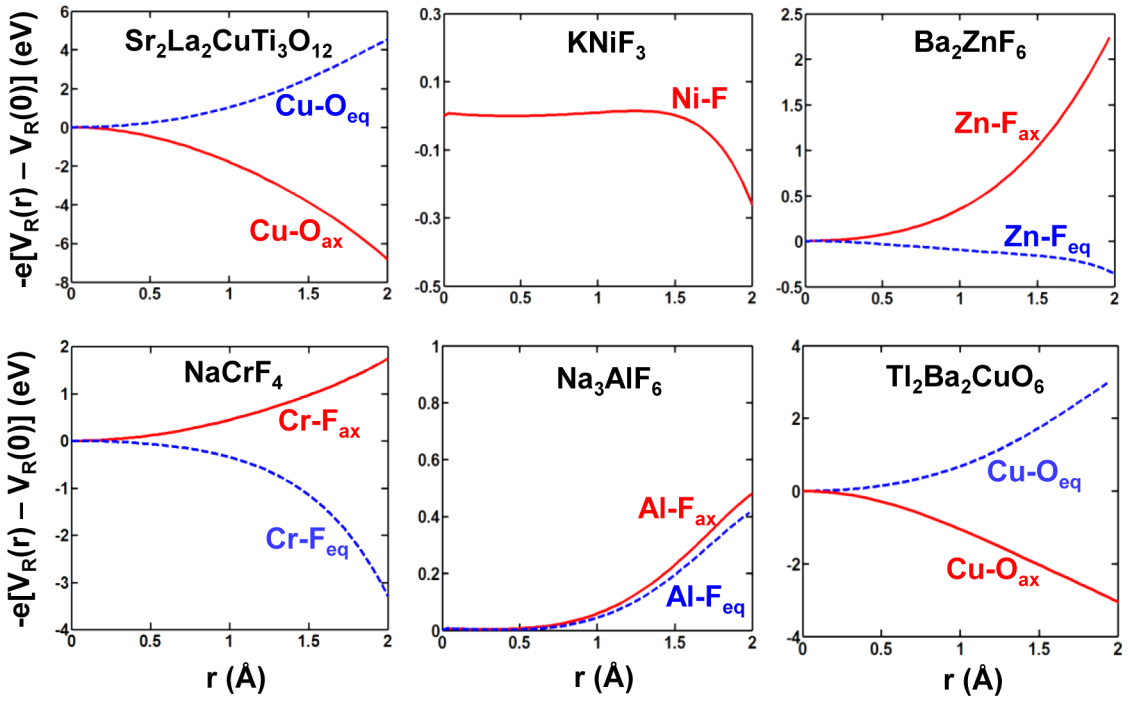

Figure 5. $(-e)\{V_R(\mathbf{r}) - V_R(0)\}$ potential energy felt by an electron of a ML_6 cluster (M = transition-metal ion; L = ligand) for various *parent* structures of orbitally ordered materials. Energies are depicted along axial M−L_{ax} (solid red lines) and in-plane equatorial M−L_{eq} (dashed blue lines) bond directions. In addition to data on several noncubic materials, the form of $(-e)\{V_R(\mathbf{r}) - V_R(0)\}$ is also depicted for the cubic $KNiF_3$ where Ni−F_{ax} and Ni−F_{eq} distances are equal.

around the F_{eq} ligand position ($r \approx 2.06$ Å). This *nonlinearity* implies that carrying out an AFD-type distortion where two Cu−F_{eq} bonds along the x (y) directions are shortened while the other two in the y (x) direction are elongated is favored from the electrostatic point of view. (b) The FD($3z^2 - r^2$) state in K_2CuF_4 generates a strong tensile strain also favoring the instability of this state. In fact in this state, the placement of two electrons in the planar antibonding $x^2 - y^2$ orbital in all Cu^{2+} ions reduces significantly the tetragonality ratio, c/a (c and a are the lattice parameters), in K_2CuF_4 when compared to other layered perovskites. To clarify this matter, geometry optimizations of K_2NiF_4 and K_2CuF_4 in the AFM ground states (using $\sqrt{2} \times \sqrt{2} \times 1$ supercells) *keeping* the K_2NiF_4 structure have been carried out. Similar calculations have been performed for La_2NiO_4 and La_2CuO_4. The obtained results give c/a values equal to 2.35 for La_2CuO_4, 2.32 for La_2NiO_4, 2.31 for K_2NiF_4, and 2.17 for K_2CuF_4. Thus, while both parent structures have similar tetragonality ratios, La_2CuO_4 has a +1.3% (compressive) strain with respect to La_2NiO_4 compared to K_2CuF_4 that displays a very large −6.1% tensile strain with respect to K_2NiF_4. Therefore, this large strain makes K_2CuF_4 in the FD($3z^2 - r^2$) state to accumulate a large elastic energy and also significantly *increases* the in-plane Cu−F_{eq} distances (2.06 Å) with respect to K_2NiF_4 (2.01 Å) *weakening* the repulsive Cu−F short-range interaction. These two facts combined with the electrostatic instability of point (a) favor the distortion of the K_2CuF_4 lattice toward an AFD state. (c) The instability of the FD($3z^2 - r^2$) state in K_2CuF_4 is also driven by the mixing of the $x^2 - y^2$ and $3z^2 - r^2$ orbitals, which contrary to K_2NiF_4, are *not equally populated*. Calculated density of states (DOS) of La_2CuO_4 and K_2CuF_4 for the *I*4/*mmm* structures, depicted in Figure 4, show that the $x^2 - y^2$ and $3z^2 - r^2$ spin−orbitals are relatively close in energy, favoring mixing when undergoing an AFD distortion that allows the deformation of the electron cloud around the Cu^{2+} ions (but not for Ni^{2+} ions) to follow the distortion. This change in hybridization can neither be described by the KK model, as ab initio calculations show that there exists *no preliminary* OO in the system, nor by the JT one, since there is no orbital degeneracy.[18,30] By contrast, the orthorhombic distortion taking place in K_2CuF_4 can be accounted for by the so-called pseudo Jahn−Teller effect where the instability is helped by changes of electronic density upon distortion when two orbitals are not equally populated.[7] A similar orthorhombic instability to that observed for K_2CuF_4 comes out in the $CuCl_4(H_2O)_4^{2-}$ complex formed in NH_4Cl.[31]

In order to test the validity of the present ideas we have calculated the frequency of the phonon at the boundary of the first Brillouin zone describing the AFD instability in layered perovskites.[14,35,36] According to our model, among K_2CuF_4, K_2NiF_4, La_2NiO_4, and La_2CuO_4, it can be expected that the lowest frequency will be displayed by K_2CuF_4 as the three factors, electrostatics, strain, and orbital occupation, favor instability. Of the other three compounds, K_2NiF_4 is the only one sharing the electrostatic properties of K_2CuF_4 and should have the next lowest frequency. Concerning the two oxides, La_2NiO_4 should have the largest frequency as none of the three effects favor a frequency softening, while in La_2CuO_4 the existence of semioccupied close-in-energy orbitals should reduce the energy of the normal mode with respect to the nickelate. Indeed, the calculated frequencies, 356i, 378, 536, and 605 cm^{-1} for K_2CuF_4, K_2NiF_4, La_2CuO_4, and La_2NiO_4, respectively, follow this pattern. To further study the magnitude of the different factors we calculated the frequency of the AFD mode in K_2CuF_4 imposing the K_2NiF_4 in-plane lattice parameter (297i cm^{-1}) and vice-versa (302 cm^{-1}). We thus find that the frequency shift associated to the strain is ∼60 cm^{-1}. Factoring the strain out and observing the strong changes in frequency occurring in the fluorides ($K_2NiF_4 \rightarrow K_2CuF_4$)

dx.doi.org/10.1021/jp412329x | J. Phys. Chem. C 2014, 118, 7554−7561

Table 2. Predictions Made Using Our Approach for a Number of Noncubic Systems Classified According to Type of Parent Lattice They Present

parent lattice	potential[a]	systems	predicted OO	experimental OO[b]
K_2NiF_4 ($I4/mmm$)	in-plane	K_2CuF_4	AFD($\sim x^2 - z^2$ /$\sim y^2 - z^2$)	AFD($\sim x^2 - z^2$ /$\sim y^2 - z^2$)
		Rb_2CuCl_4	AFD($\sim x^2 - z^2$ /$\sim y^2 - z^2$)	AFD($\sim x^2 - z^2$ /$\sim y^2 - z^2$)
		Cs_2AgF_4	AFD($\sim x^2 - z^2$ /$\sim y^2 - z^2$)	AFD($\sim x^2 - z^2$ /$\sim y^2 - z^2$)
La_2NiO_4 ($I4/mmm$)	out-of-plane	La_2CuO_4	FD($x^2 - y^2$)	FD($x^2 - y^2$)
Ba_2ZnF_6 ($I4/mmm$)	in-plane	Ba_2CuF_6	AFD($\sim x^2 - z^2$ /$\sim y^2 - z^2$)	AFD($\sim x^2 - z^2$ /$\sim y^2 - z^2$)
$NaCrF_4$ ($P4/mmm$)	in-plane	$NaMnF_4$	AFD($\sim 3x^2 - r^2$ /$\sim 3y^2 - r^2$)[c]	AFD($\sim 3x^2 - r^2$ /$\sim 3y^2 - r^2$)[c]
$Sr_2La_2CuTi_3O_{12}$ ($P4/mmm$)	out-of-plane	$Sr_2La_2CuTi_3O_{12}$	FD($x^2 - y^2$)	FD($x^2 - y^2$)
		$Ca_2La_2CuTi_3O_{12}$	FD($x^2 - y^2$)	FD($x^2 - y^2$)
$Tl_2Ba_2CuO_6$ ($I4/mmm$)	out-of-plane	$Tl_2Ba_2CuO_6$	FD($x^2 - y^2$)	FD($x^2 - y^2$)

[a]Using the structure of the parent lattice, the type of potential $V_R(\mathbf{r})$ experienced over the magnetic complex is determined (see Figure 3) and classified according to in-plane and out-of-plane. [b]According to the type of field, the expected orbital ordering is compared with the experimental orbital ordering found in the system (see Supporting Information for experimental data). [c]Change in notation for $NaMnF_4$ is due to the fact that in this system the $3z^2 - r^2/x^2 - y^2$ orbitals contain 1 electron instead of the 3 found in Cu^{2+} systems (see main text).

compared to the oxides ($La_2NiO_4 \rightarrow La_2CuO_4$) we see that the in-plane deformation of the electronic cloud in copper lattices is strongly influenced by the electrostatic field. We would like to note that in all our calculations we find that the AFD distortion frequency is always more unstable for the FM state than the AFM one. This is consistent with experimental data, the Goodenough–Kanamori rules,[37] and our previous results[32] for ferroelectric and octahedral rotation distortions.

Because of the instability of the FD($3z^2 - r^2$) state in K_2CuF_4 there are two different in-plane Cu–F distances, equal to 2.223 and 1.900 Å.[32,33] However, despite the existence of this significant in-plane distortion the present calculations prove that the hole orbital *still* has a *dominant* $3z^2 - r^2$ character. More precisely, if we write the wave function of the orbital where the unpaired electron is located as

$$|\phi_H\rangle = \alpha|3z^2 - r^2\rangle + \beta|x^2 - y^2\rangle \quad (1)$$

the present calculations give $\alpha^2/\beta^2 \approx 5$. This relevant fact, is consistent with the ^{19}F nuclear magnetic resonance data by Yamada[27] suggesting that the hole in K_2CuF_4 is located in a mainly $3z^2 - r^2$ orbital. Along this line the experimental g-shift when the magnetic field is parallel to **c** axis is[27] $g_c - g_0 = 0.08$, again consistent with a hole in a mainly $3z^2 - r^2$ orbital.[27,31]

The electronic structure of K_2CuF_4 has often been explained considering an *isolated* CuF_6^{4-} complex under the nearly tetragonal distortion described by the experimental values R_L = 2.223 Å and $R_S \cong 1.92$ Å. In this situation the main axis for an *isolated* CuF_6^{4-} complex would be in the plane perpendicular to the **c** axis, and the hole would reside in $\sim x^2 - z^2/\sim y^2 - z^2$ orbitals. Such orbitals can be viewed as 75% of $3z^2 - r^2$ and 25% of $x^2 - y^2$, thus implying $\alpha^2/\beta^2 = 3$. The present results and the calculated value $\alpha^2/\beta^2 \approx 5$ stress that the character of the hole in K_2CuF_4 can hardly be understood without considering the effects of the electrostatic potential that favors its localization on the axial orbital $3z^2 - r^2$ and thus limits α^2/β^2 to be necessarily higher than 3.

For clearing up this matter it is worth considering the electron paramagnetic resonance results performed on $KZnF_3$:Cu^{2+}, where elongated CuF_6^{4-} complexes are formed due to a static Jahn–Teller effect.[34,18] As in the case of a perovskite lattice like $KZnF_3$ where the $V_R(\mathbf{r})$ potential is almost flat (see Figure 5 for the similar $KNiF_3$ perovskite), the results on CuF_6^{4-} in $KZnF_3$:Cu^{2+} can reasonably be understood in terms of isolated complexes. When the magnetic field is perpendicular to the main local axis in $KZnF_3$:Cu^{2+} it is measured[34] $g_\perp - g_0 = 0.14$. Thus, the comparison of this figure with $g_c - g_0 = 0.08$ measured[27] for K_2CuF_4 again supports that the amount of the $3z^2 - r^2$ character of the hole in K_2CuF_4 is higher than 80%. According to these results the wave function of the hole in K_2CuF_4 is primarily determined by the electrostatic potentials, $V_R(\mathbf{r})$, felt in the parent structure, while the small amount of $x^2 - y^2$ character is induced by the subsequent orthorhombic distortion. A similar situation to this one has been proved for the $CuCl_4(H_2O)_4^{2-}$ complex formed in NH_4Cl.[31] Thus, according to the present view although equilibrium situation for K_2CuF_4 is usually denoted as AFD($\sim x^2 - z^2/\sim y^2 - z^2$) it should better be described as AFD($\sim 3z^2 - r^2$).

Application to Other Noncubic Compounds. Finally, we will discuss the range of application of the present ideas to other systems given in Table 2 and Figure 5 (see Supporting Information for more details on structural parameters).

It is clear that the model cannot be applied to lattices where the electrostatic potential $V_R(\mathbf{r})$ is almost isotropic, and thus, it does not induce any splitting on the $3z^2 - r^2/x^2 - y^2$ orbitals of the transition metal complex. In such situations the traditional JT and KK models are dominant. This is the case of cubic lattices as the perovskite $KNiF_3$ ($Pm3m$ group) where the $V_R(\mathbf{r})$ potential is almost flat and equivalent along the three *x*, *y*, and *z* directions (Figure 5). Similarly, the $V_R(\mathbf{r})$ potential is almost isotropic in some noncubic lattices like, for example, Na_3MnF_6 whose parent compound is Na_3AlF_6 (Figure 5).

However, there are many other systems where the form of the $V_R(\mathbf{r})$ potential for the parent structure already provides us with relevant information on the orbital ordering. For example, in Figure 5 we show the potential for $NaCrF_4$ (space group $P4/mmm$), which is just the parent crystal of $NaMnF_4$ involving high-spin ($S = 2$) Mn^{3+} cations (d^4 electronic configuration) and one unpaired σ-electron. Experimentally, the $NaMnF_4$ compound displays an antiferrodistortive state (Table 2). The picture given by the electrostatic potential corresponding to the parent structure of $NaMnF_4$ is fully consistent with that of K_2NiF_4, also shown in Figure 5. In both lattices there is a strong decrease of the potential along the ⟨100⟩ directions and a moderate increase along [001] favoring a localization of the unpaired σ-electron in a FD($x^2 - y^2$) state with two holes in $3z^2 - r^2$. Because of the form of $V_R(\mathbf{r})$ in the parent crystal of $NaMnF_4$ the energy of the σ-electron is decreased by increasing the equatorial metal–ligand distance, thus favoring in principle a compressed situation. Similarly to what happens for K_2CuF_4,

dx.doi.org/10.1021/jp412329x | J. Phys. Chem. C 2014, 118, 7554–7561

this state is unstable experiencing a pseudo JT distortion making that the final equilibrium state an AFD($\sim 3x^2 - z^2/\sim 3y^2 - z^2$) state pointing out that these orbitals have a dominant $x^2 - y^2$ character. However, a system like the quadruple perovskite $Sr_2La_2CuTi_3O_{12}$ ($P4/mmm$ group) shows a strongly descending potential along the z direction (Figure 5), which favors an electrostatically stable FD($x^2 - y^2$) state, a fact that is also in agreement with experiment. Looking at Table 2 we see that many systems follow these general criteria. Thus, and because of the diverse nature of the systems, with transition metals (M = Cu^{2+}, Mn^{3+}, Ni^{3+}, Ag^{2+}, etc.) and ligands (L = O^{2-}, F^-, Cl^-, etc.) of very different chemical nature where the present ideas can be applied, we believe that the simple inspection of the $V_R(\mathbf{r})$ potential can provide crucial information to understand the actual origin of the OO in many noncubic systems.

IV. CONCLUSIONS

In summary, we have shown that in systems that do not have a cubic parent structure (like layered perovskites) and where usual Kugel–Khomskii and Jahn–Teller models cannot be strictly applied, the nature of the orbital ordering and its associated structure is mainly driven by the internal electric field over the active electrons localized in the complex, a fact that is usually ignored in the realm of solid-state chemistry.

We would like to stress here the novelty of our explanation for OO in noncubic systems. Previous approaches, ranging from model Hamiltonians (see, e.g., ref 33) to first-principles-based approaches (e.g., ref 38), use "*crystal-field splitting*" terms that contain implicitly the electrostatic contribution described above. However, these terms are treated either in an *effective* way, i.e., finding the gap between the d-levels using ab initio calculations without separating the local covalent contribution from the long-range from $V_R(\mathbf{r})$ or simply in a phenomenological way,[36] with parameters being adjusted or varied over a range of values so that the Hamiltonian's solution reproduces the experimental properties. Therefore, they are not used in the way employed here that both explains qualitatively the sign of the splitting, determining the kind of orbital ordering, and allowing the prediction of a trend between different systems.

As the relevance of the internal electric field for understanding the actual OO in many noncubic systems has been proved by the present study it opens a window for improving the design of insulating materials with particular orbital ordering patterns.

Finally, it is worth nothing here that the internal electric field considered in this work substantially alters the positions of the d–d transitions of Cu^{2+} complexes in insulating lattices[18] and therefore plays also an important role in the spectroscopy of other systems, explaining, for instance, the different color displayed by gemstones like ruby, alexandrite, or emerald.[39,40] In this sense it is has been shown that in K_2CuF_4 the often ignored $V_R(\mathbf{r})$ potential induces changes on the energy of 3d levels, which are, at least, 1 order of magnitude higher than those due to superexchange interactions.

■ ASSOCIATED CONTENT

Supporting Information

Details on the structure and electrostatic potentials for several families of fluorides and oxides. This material is available free of charge via the Internet at http://pubs.acs.org.

■ AUTHOR INFORMATION

Corresponding Author

*(P.G.-F.) Phone: +34-942202069. E-mail: garciapa@unican.es.

Notes

The authors declare no competing financial interest.

■ ACKNOWLEDGMENTS

This work has been supported by the Spanish Ministerio de Ciencia y Tecnología under Projects FIS2012-30996 and FIS2012-37549-C05-4.

■ REFERENCES

(1) Hwang, H. Y.; Iwasa, Y.; Kawasaki, M.; Keimer, B.; Nagaosa, N.; Tokura, Y. Emergent Phenomena at Oxide Interfaces. *Nat. Mater.* **2012**, *11*, 103–113.

(2) Zubko, P.; Gariglio, S.; Gabay, M.; Ghosez, P.; Triscone, J.-M. Interface Physics in Complex Oxide Heterostructures. *Annual Rev. Condens. Matter Phys.* **2011**, *2*, 141–161.

(3) Tokura, Y.; Nagaosa, N. Orbital Physics in Transition-Metal Oxides. *Science* **2000**, *288*, 462–468.

(4) Cheong, S.-W. Transition Metal Oxides: The Exciting World of Orbitals. *Nat. Mater.* **2007**, *6*, 927–928.

(5) Kanamori, J. Crystal Distortion in Magnetic Compounds. *J. Appl. Phys.* **1960**, *31*, S14–S23.

(6) Halperin, B.; Englman, R. Cooperative Dynamic Jahn–Teller Effect. II. Crystal Distortion in Perovskites. *Phys. Rev. B* **1971**, *3*, 1698–1708.

(7) Bersuker, I. B. *The Jahn–Teller Effect*; Cambridge University Press: Cambridge, U.K., 2006.

(8) Kugel, K. I.; Khomskii, D. I. Crystal Structure and Magnetic Properties of Substances with Orbital Degeneracy. *Sov. Phys. JETP* **1973**, *37*, 725–730.

(9) Kugel, K. I.; Khomskii, D. I. The Jahn–Teller Effect and Magnetism: Transition Metal Compounds. *Sov. Phys. Usp.* **1982**, *25*, 231–256.

(10) Rodríguez-Carvajal, J.; Hennion, M.; Moussa, F.; Moudden, A. H. Neutron-Diffraction Study of the Jahn–Teller Transition in Stoichiometric $LaMnO_3$. *Phys. Rev. B* **1998**, *57*, R3189–R3192.

(11) Okazaki, A. The Polytype Structures of $KCuF_3$. *J. Phys. Soc. Jpn.* **1969**, *26*, 870–870.

(12) Pavarini, E.; Koch, E.; Lichtenstein, A. I. Mechanism for Orbital Ordering in $KCuF_3$. *Phys. Rev. Lett.* **2008**, *101*, 266405.

(13) Pavarini, E.; Koch, E. Origin of Jahn–Teller Distortion and Orbital Order in $LaMnO_3$. *Phys. Rev. Lett.* **2010**, *104*, 086402.

(14) Hidaka, M.; Inoue, K.; Yamada, I.; Walker, P. J. X-ray Diffraction Study of the Crystal Structures of K_2CuF_4 and $K_2Cu_xZn_{1-x}F_4$. *Phys. B* **1983**, *121*, 343–350.

(15) Hord, R.; Cordier, G.; Hoffmann, K.; Buckow, A.; Pascua, G.; Luetkens, H.; Alff, L.; Albert, B. Enhanced Two-dimensional Behavior of Metastable T′-La_2CuO_4, the Parent Compound of Electron-Doped Cuprate Superconductors. *Phys. Rev. B* **2010**, *82*, 180508.

(16) Mostovoy, M. V.; Khomskii, D. I. Orbital Ordering in Charge Transfer Insulators. *Phys. Rev. Lett.* **2004**, *92*, 167201.

(17) Brzezicki, W.; Oles, A. M. Entangled Spin-Orbital Phases in the d^9 Model. *Acta Phys. Pol., A* **2012**, *121*, 1045–1047. Sachdev, S. Colloquium: Order and Quantum Phase Transitions in the Cuprate Superconductors. *Rev. Mod. Phys.* **2003**, *75*, 913–932.

(18) García-Fernandez, P.; Barriuso, M. T.; García-Lastra, J. M.; Moreno, M.; Aramburu, J. A. *J. Phys. Chem. Lett.* **2013**, *4*, 2385–2390.

(19) CRYSTAL code: Dovesi, R.; Civalleri, B.; Orlando, R.; Roetti, C.; Saunders, V. R. *Rev. Comput. Chem.* **2005**, *21*, 1–125.

(20) Bilc, D. I.; Orlando, R.; Shaltaf, R.; Rignanese, G.-M.; Íñiguez, J.; Ghosez, Ph. Hybrid Exchange-Correlation Functional for Accurate Prediction of the Electronic and Structural Properties of Ferroelectric Oxides. *Phys. Rev. B* **2008**, *77*, 165107.

(21) Bredow, T.; Gerson, A. Effect of Exchange and Correlation on Bulk Properties of MgO, NiO, and CoO. *Phys. Rev. B* **2000**, *61*, 5194−5201.
(22) Garcia-Fernandez, P.; Ghosh, S.; English, N. J.; Aramburu, J. A. Benchmark Study for the Application of Density Functional Theory to the Prediction of Octahedral Tilting in Perovskites. *Phys. Rev. B* **2012**, *86*, 144107.
(23) Maslyuk, V. V.; Islam, M. M.; Bredow, T. Electronic properties of compounds of the Li_2O-B_2O_3 system. *Phys. Rev. B* **2005**, *72*, 125101.
(24) CRYSTAL Basis Sets Library, see crystal web page.
(25) We employed nominal charges in most of our calculations but adequate prediction of the OO state in systems containing nominally highly charged (4+, 5+, 6+) cations or with strong covalency requires the use of first-principles-calculated charges, as shown in ref 18.
(26) Garcia-Fernandez, P.; Trueba, A.; Barriuso, M. T.; Aramburu, J. A.; Moreno, M. Tunneling Splitting of Jahn−Teller Ions in Oxides. *Phys. Rev. Lett.* **2010**, *104*, 035901.
(27) Yamada, I. Magnetic Properties of K_2CuF_4: A Transparent Two-Dimensional Ferromagnet. *J. Phys. Soc. Jpn.* **1972**, *33*, 979−988.
(28) Caciuffo, R.; Paolasini, L.; Sollier, A.; Ghigna, P.; Pavarini, E.; van den Brink, J.; Altarelli, M. Resonant X-ray Scattering Study of Magnetic and Orbital Order in $KCuF_3$. *Phys. Rev. B* **2002**, *65*, 174425.
(29) Reinen, D. The Modulation of Jahn−Teller Coupling by Elastic and Binding Strain Perturbations: A Novel View on an Old Phenomenon and Examples from Solid-State Chemistry. *Inorg. Chem.* **2012**, *51*, 4458−4472.
(30) Aramburu, J. A.; Garcia-Lastra, J. M.; Garcia-Fernandez, P.; Barriuso, M. T.; Moreno, M. *Inorg. Chem.* **2013**, *52*, 6923−6933.
(31) Garcia-Fernandez, P.; García-Lastra, J. M.; Trueba, A.; Barriuso, M. T.; Aramburu, J. A.; Moreno, M. Insulators Containing $CuCl_4X_2^{2-}$ (X = H_2O, NH_3) units: Origin of the Orthorhombic Distortion Observed Only for $CuCl_4(H_2O)_2^{2-}$. *Phys. Rev. B* **2012**, *85*, 094110−1−9.
(32) Garcia-Fernandez, P.; Aramburu, J. A.; Moreno, M. Influence of Magnetic Ordering on Structural Instabilities in Insulating Perovskites. *Phys. Rev. B* **2011**, *83*, 174406.
(33) Brzezicki, W.; Olés, A. M. Entangled Spin-Orbital Phases in the Bilayer Kugel−Khomskii Model. *Phys. Rev. B* **2011**, *83*, 214408.
(34) Dubicki, L.; Riley, M. J.; Krausz, E. R. Electronic Structure of the Copper(II) Ion Doped in Cubic $KZnF_3$. *J. Chem. Phys.* **1994**, *101*, 1930−1939.
(35) Friebel, C.; Reinen, D. Z . Existieren tetragonal gestauchte Koordinationsoktaeder mit zweiwertigem Kupfer? *Anorg. Allg. Chem.* **1974**, *407*, 193−200.
(36) Riley, M. J.; Dubicki, L.; Moran, G.; Krausz, E. R.; Yamada, I. Optical Spectrum of Dipotassium Tetrafluorocuprate. *Inorg. Chem.* **1990**, *29*, 1614−1626.
(37) Goodenough, J. B. Theory of the Role of Covalence in the Perovskite-Type Manganites [La, M(II)]MnO_3. *Phys. Rev.* **1955**, *100*, 564.
(38) Gorelov, E.; Karolak, M.; Wehling, T. O.; Lechermann, F.; Lichtenstein, A. I.; Pavarini, E. Nature of the Mott Transition in Ca_2RuO_4. *Phys. Rev. Lett.* **2010**, *104*, 226401.
(39) Aramburu, J. A.; Garcia-Fernandez, P.; Garcia-Lastra, J. M.; Barriuso, M. T.; Moreno, M. Internal Electric Fields and Color Shift in Cr^{3+}-based Gemstones. *Phys. Rev. B* **2012**, *85*, 245118.
(40) Garcia-Lastra, J. M.; Aramburu, J. A.; Barriuso, M. T.; Moreno, M. Optical Properties of Cr^{3+}-doped Oxides: Different Behavior of Two Centers in Alexandrite. *Phys. Rev. B* **2006**, *74*, 115118−1−5.